EFFECT OF INJECTION AND NONUNIFORMITY OF TEMPERATURE ON FRICTION IN THE ENTRY REGION OF A TUBE

A. V. Fafurin

UDC 532.526

Results are presented from an experimental study of the effect of injection and temperature nonuniformity on the coefficient of friction in the entry region of a tube. A method is proposed whereby the kinematic flow characteristics can be used to determine the coefficient of friction directly from experimental data. This method has been applied to the data of various authors. The results of experiments carried out over a wide range of conditions are reported.

Coefficients of friction can be determined experimentally either by using floating elements to directly measure tangential shear stresses, or by having recourse to indirect procedures involving treatment of the velocity profile or numerical integration of the momentum relation. Methods based on electrochemical principles and thermal analogies have also found wide application.

Resort is usually had to indirect methods since it is not always possible to measure the tangential stresses directly, especially under complex gasdynamic conditions.

Two procedures are available for finding the coefficient of friction from the velocity profile in the turbulence center of the boundary layer [1, 2]. The first of these rests on the existence of a logarithmic region within the boundary layer. Here a velocity profile in the coordinates $w_x/w_0 = f(w_0 y/\nu)$ is developed, and the equation

$$w_x = V_+ \varkappa^{-1} (\ln y + \text{const}) \tag{1}$$

is then used to find the coefficient of friction.

The value obtained for the coefficient of friction will depend on the coefficient of turbulence $\varkappa$, and its accuracy will vary with the precision of measurement of the slope (V_+). The drawback to this method lies in the fact that it cannot be applied to gradient and nonstationary flow where the logarithmic region in the velocity profile shrinks away to essentially zero [3]. The method proposed in [2] is largely an improved version of this procedure, and suffers from the same defects.

The coefficient of friction can also be obtained from the integral momentum equation. Here the precision of the result obtained is largely determined by the accuracy of the velocity profile measurements and subsequent logitudinal integration and differentiation.

The work of [3, 4] was carried out with a momentum equation of the form

$$-\tau_w \frac{r_0}{\cos\alpha}\, dx = d \int_0^{r_0 \cos^{-1}\alpha} \rho w_x^2 r\, dy + d \int_0^{r_0 \cos^{-1}\alpha} \Pr dy \tag{2}$$

The accuracy of the final result was thereby improved, the first term on the right-hand side of this equation being generally much smaller than the second, without, of course, eliminating the error inherent in velocity profile measurements. In Eqs. (1) and (2), w_x designates the velocity, P the pressure, r the radius, ρ the density, V_+ the dynamic velocity, and τ_w the tangential stress on the wall, while x and y are the

Kazan'. Translated from Zhurnal Prikladnoi Mekhaniki i Tekhnicheskoi Fiziki, No. 1, pp. 42-48, January-February, 1974. Original article submitted December 14, 1972.

respective longitudinal and transverse coordinates, and α is the angle between the channel axis and the wall.

By drawing on the relation between kinematic and integral flow characteristics it should be possible to eliminate the necessity of velocity profile measurements thereby considerably increasing the accuracy of the final result.

This relation can be developed from the continuity equation and the integral displacement thickness equation for the axially symmetric channel.

Here one has

$$\partial \rho w_x r / \partial x + \partial \rho w_r r / \partial r = 0 \tag{3}$$

$$\frac{\delta^+}{r_0} = \int_0^1 \left(1 - \frac{\rho w_x}{\rho_0 w_0}\right)\left(1 - \frac{y \cos \alpha}{r_0}\right) d\left(\frac{y}{r_0}\right) \tag{4}$$

Integration of (3) over the range of variation of the longitudinal and transverse coordinates gives

$$\rho_0 w_0 \bar{r}_0^2 (1 - 2\delta^+ \cos \alpha / r_0) = \rho_{01} w_{01} (1 - 2\delta_1^+ \cos \alpha_1 / r_{01}) + \int_{X_1}^{X_i} \rho w_W \frac{\bar{r}_0}{\cos \alpha} dX \tag{5}$$

Let it now be assumed that

$$\rho w_x / \rho_0 w_0 = (y / r_0)^n \tag{6}$$

n being an unknown empirical constant, and $\bar{r}_0 = r_0/r_{01}$.

Substituting from (6) into (4) and integrating, one finds that

$$\frac{\delta^+}{r_0} = \frac{n^2 (2 - \cos \alpha) + n (4 - \cos \alpha)}{2n^2 + 6n + 4} \tag{7}$$

Equation (7) can now be solved for n to obtain

$$n = -\frac{6\delta^+ / r_0 - 4 + \cos \alpha}{2(2\delta^+ / r_0 - 2 + \cos \alpha)} + \left[\frac{1}{4}\left\{\frac{6\delta^+ / r_0 - 4 + \cos \alpha}{2\delta^+ / r_0 - 2 + \cos \alpha}\right\}^2 - \frac{4\delta^+ / r_0}{2\delta^+ / r_0 - 2 + \cos \alpha}\right]^{1/2} \tag{8}$$

For flow in a constant-cross-section tube, r_0 = const, $\cos \alpha = 1$, so that (8) reduces to

$$n = -\frac{3}{2} + \left[\left(\frac{1}{2}\frac{\delta^+}{r_0} - \frac{9}{4}\right)\left(2\frac{\delta^+}{r_0} - 1\right)^{-1}\right]^{1/2} \tag{9}$$

Solving (4) for the displacement thickness, one finds that

$$\frac{\delta^+}{r_0} = \frac{1}{2 \cos \alpha}\left\{1 - \frac{1}{\rho_0 w_0 \bar{r}_0^2}\left[\rho_{01} w_{01}\left(1 - 2\frac{\delta_1^+ \cos \alpha_1}{r_{01}}\right) + 4\int_0^{X_i} \rho w_W \frac{\bar{r}_0 \, dX}{\cos \alpha}\right]\right\} \tag{10}$$

By measuring the dynamic pressure distribution and the transverse flux, and drawing on Eqs. (8) and (10), the exponent of (6) can be evaluated for any particular section. The form of Eq. (6) is such as to limit application to cases of breakaway flow.

For flow in the entry region of a tube, simultaneous solution of (9) and (10) gives the following simple expression for n

$$n = -{}^3/_2 + \left[\frac{1}{4} + 2\frac{\rho_0 w_0}{\rho_{01} w_{01}}\right]^{1/2} \tag{11}$$

Integration of (2) over the working section gives

$$\int_{X_1}^{X_i} \tau_w \bar{r}_0 \frac{dx}{\cos \alpha} = -\frac{\beta_1}{4}\rho_{01} w_{01}^2 \left(\bar{r}_{0i}^2 \frac{\rho_0 w_{0i}^2}{\rho_{01} w_{01}^2}\frac{\beta_i \cos \alpha_1}{\beta_1 \cos \alpha_i}\right) - \frac{P_1}{4 \cos \alpha_1}\left(\bar{r}_{0i}^2 \frac{P_i}{P_1}\frac{\cos \alpha_1}{\cos \alpha_i} - 1\right) \tag{12}$$

$$\beta_i = 2\int_0^1 \frac{\rho w_x^2}{\rho_0 w_0^2} d\left(\frac{r}{r_0}\right)^2 \tag{13}$$

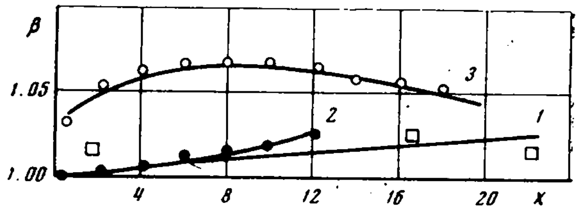

Fig. 1

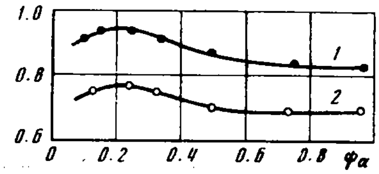

Fig. 2

β_1 being the momentum flux parameter.

In the case of nonisothermal streamline flow of a permeable surface, (13) can be integrated directly by drawing on (6) and relations following from field similarity for the dimensionless enthalpy, concentration, and velocity, i.e.,

$$\rho / \rho_0 = [\psi_c + (1 - \psi_c)\,\omega]\{[\psi_h + (1 - \psi_h)\omega][\psi_g + (1 - \psi_g)\,\omega]\}^{-1}$$

Here ψ_c, ψ_g, and ψ_n are the respective heat capacity, nonuniformity, and enthalpy factors, and $\omega = w_x/w_0$.

It will be shown below that this approach gives a reasonably accurate estimate of the momentum flux parameter.

Let us at the moment simply compare values of the momentum flux parameter obtained through these various procedures.

Figure 1 gives a comparison of the results obtained by graphical integration [4, 5] of the experimental data and by the methods outlined in the present work. The points of curves 1 and 3 indicate values of the momentum flux parameter obtained either from velocity profiles developed over various sections of the entry region of a hydraulically smooth tube [4], or from profiles obtained under transverse gas flow in the main portion of the tube [5].

Results obtained by the method of the present paper are covered by the curve of Figs. 1. The exponent n of (6) was evaluated from Eqs. (9) and (10). In each case, the velocity distribution along the tube axis was taken from the published graphs of [4, 5]. The results obtained are seen to be in satisfactory agreement in every instance. Inadequacies in the method and inaccuracies in the experimental data might both account for discrepancies in the neighborhood of $x \sim 0$. The errors of measurement and velocity profile treatment are minor over the entry region of hydrodynamic stabilization where the boundary layer is thin. Additional difficulties arise here from the fact that the momentum flux parameter varies by as much as 3% under the conditions of [4].

The points on curve 2 of Fig. 1 represent the results of treatment of data obtained in the entry region of a rough-walled tube, again using the methods outlined in the present paper [6]. The experimental values are seen to be in satisfactory agreement with values obtained by integrating (13), where the working equation for β takes the form

$$\beta = 2\frac{\delta}{r_0}\left\{1 - 5\sqrt{\frac{c_f}{2}} + \frac{\delta}{r_0}\left(\frac{87.5}{8}\frac{c_f}{2} + \frac{5}{4}\sqrt{\frac{c_f}{2}} - \frac{1}{2}\right)\right\} + 1 - \left(\frac{\delta}{r_0}\right)^2 \qquad (14)$$

Here it was assumed that $\varkappa = 0.4$. The coefficient of friction, the thickness of the boundary layer, and the relative velocity along the tube axis, quantities required for substitution in (14), were determined by the methods of [6].

Measurements on high-enthalpy gas flow [3, 7, 8] have shown that temperature nonuniformity results in no more than a slight deformation of the flow profile across a boundary layer. This suggests the possibility of extending the method proposed here to still more complex cases.

Let us therefore now assume entropy and velocity field similarity in the nonisothermal turbulent boundary layer, and, on this basis, integrate Eq. (13).

Drawing on (6), one obtains

$$\beta = \int_0^1 \frac{\psi_\alpha \xi^{2n}(1 - \xi\cos\alpha)\cos\alpha\, d\xi}{1 - (1 - \psi_\alpha)\xi^n}$$

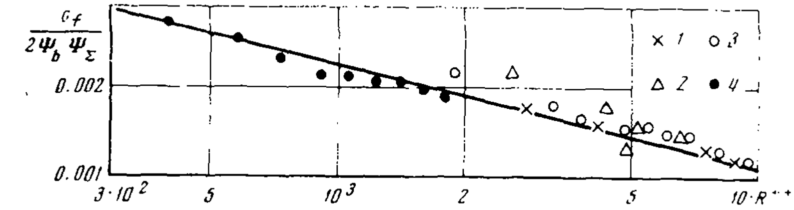

Fig. 3

$$\psi_\Sigma = \frac{\psi_h}{1-\Sigma\alpha_i\psi_i^\circ}, \quad \psi_h = \frac{h_w}{h_1}, \quad \psi_i^\circ = \frac{h_i}{h_0} \tag{15}$$

The curves of Fig. 2 (for 1, $\langle\rho w\rangle/\rho_0 w_0$; for 2, β) cover the results obtained by treating the data of [3] through Eqs. (11) and (15), while the points indicate results obtained from a graphical integration of (13), using experimental data on the velocity profile and temperature across the boundary layer in the region of stabilized flow. The effect of temperature nonuniformity on the relative axial velocity was taken from [3]. The results obtained by these two procedures are in satisfactory agreement.

Thus the momentum flux parameter for gas flow with transverse mass transport in a rough-walled tube under nonisothermal conditions can be obtained from a measurement of the velocity at the outer boundary layer edge and the mean velocity averaged over the cross section in question.

The values of β obtained here were used, in turn, to obtain a solution to Eq. (12). Using the method of least squares, the drag integral was approximated as an m-term polynomial series,

$$\int_{X_1}^{X_i} \tau_w \bar{r}_0 \frac{dX}{\cos\alpha} = \sum_0^m a_i X^i \tag{16}$$

The value of the coefficient of friction was then obtained by differentiating (16)

$$\frac{c_f}{2} = \sum_1^m i a_i X^{i-1} \cos\alpha\, [\bar{r}_0 \rho_0 w_{0i}^2]^{-1} \tag{17}$$

In order to establish the frictional law, it is necessary to have Reynolds numbers determined from the momentum transfer thickness. Here one has recourse to the equation for the conservation of momentum, written as

$$\frac{dR^{++}}{dX} + \frac{R^{++}}{W_0}\frac{dW_0}{dX}(1+H) + \frac{R^{++}}{r_0}\frac{dr_0}{dX} - \frac{R}{4\rho_0 w_0^2\cos\alpha}\frac{dP_0^*}{dX} = \frac{c_f}{2} W_0 R_1 (1+b_1)$$
$$R^{++} = \frac{\rho_0 w_0 \delta^{++}}{\mu}, \quad H = \frac{\delta^+}{\delta^{++}}, \quad W_0 = \frac{w_0}{w_{01}} \tag{18}$$
$$R = \frac{\rho_0 w_0 D}{\mu}, \quad b_1 = \frac{\rho_w w}{\rho_0 w_0}\frac{2}{c_f}, \quad X = x/2r_0$$

with the subscript 0 designating quantities evaluated at the outer boundary layer edge and 1 quantities evaluated at the channel entrance; w the wall parameter, and P* the total pressure.

Integration of (18) gives

$$R_i^{++} = \exp\left\{-\int_{w_{01}}^{w_{0i}} \frac{1+H}{w_0}\,dw_0 - \ln\frac{r_{0i}}{r_{01}}\right\}\left[\int_{X_1}^{X_i}\left(\frac{c_f}{2} W_0 R_1 (1+b_1) + \frac{R}{4\rho_0 w_0^2\cos\alpha}\frac{dP_0^*}{dX}\right)\exp\left(\int_{w_{01}}^{w_0}\frac{1+H}{w_0}\,dw_0 + \ln\frac{r_{0i}}{r_{01}}\right)dX + R_1^{++}\right] \tag{19}$$

Figure 3 shows the results of treating experimental data (1, [4]; 2, [5]; 3, 4, [6]) on friction in the entry region and principal section of tubes, both smooth and rough walled, under transverse gas flow. The starting point for this work was the measured axial velocity, and the mean velocity averaged over the section in question.

The experimental data were treated in the following manner. The displacement thickness was first calculated from Eq. (10) using the measured kinematic flow characteristics for the cross section in ques-

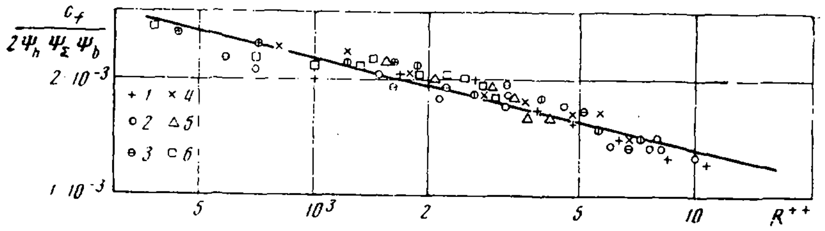

Fig. 4

tion and for entry at that segment of the tube under study. The exponent of (6) was then obtained from Eq. (8).

The complex quantity β was then calculated from Eq. (15). The value of the drag integral was found as a function of the longitudinal coordinate, using Eq. (12). The method of least squares was used to carry the resulting sequence into a series of the type of (16), and the coefficient of friction then obtained by differentiating the latter. The value of the Reynold's number could be obtained by numerical integration of (19).

The value of the coefficient of friction was reduced to standard conditions by the use of various functions, each covering one type of interaction.

Thus the effect of surface roughness was allowed for by introducing the function

$$\Psi_r = \left(\frac{\varkappa\eta_{10} - \ln \xi_{10}}{\varkappa\eta_1 - \ln \xi_1}\right)^2, \quad \Psi_r = \left(\frac{c_f}{c_{f0}}\right)_{R^{++}} \tag{20}$$

derived earlier in [6], and the effect of injection by the function

$$\Psi_c = \left(1 - \frac{b}{b_c}\right)^2, \quad b_c = 4\left(1 + \frac{0.83}{R^{++0.14}}\right) \tag{21}$$

derived in [9].

It is seen from the graph that the experimental points clustered around a curve satisfying the equation

$$c_f / 2 = 0.0128 \Psi_\Sigma R^{++-0.25} \quad \Psi_\Sigma = \Pi \Psi_i \tag{22}$$

The problem of heat exchange in the entry region of a tube under nonisothermal conditions and with injection has been discussed earlier in [7, 10, 11] where measured values of the local axial flux and the mean velocity over the streaming surface are reported. The methods of the present paper can be used to obtain the coefficient of friction from measurements of this type.

The results obtained from frictional data applying to the entry region of the tube under various types of departure from temperature uniformity (1, $\psi_h = 0.8$; 2, 0.61; 3, 0.58; 4, 0.56), are shown in Fig. 4. Here the coefficient of friction was calculated from Eqs. (12), (15), and (17), and the Reynolds number obtained from (19). The coefficient of roughness was evaluated from (2), and the departure from isothermal conditions expressed through

$$\psi_h = 1 + [4(1 - \sqrt{\Psi_h})][\Psi_h(1 - \alpha_0 \sqrt{\Psi_h \psi_h c_{f0}/2})]^{-1} \tag{23}$$

The crest height relative to the roughness was obtained from the measured drag coefficient and the Nikuradze formula [13], and proved to be 10^{-3}. The drag coefficient was obtained by means of a preliminary scavenging of the main portion of the tube. It is obvious that the points fell around a curve of the type of (22) with $\Psi_\Sigma = 1$.

The figure also contains points obtained over the hydrodynamic stabilization segment of the tube, working under nonisothermal conditions with injection (5, $\psi_h = 0.6$; $b = 3.3$; 6, $\psi_h = 0.76$, $b = 0.96$) [10, 11].

Here treatment of the data proceeded through Eqs. (9), (10), (12), (15), and (19).

The values obtained for the coefficient of friction were reduced to standard conditions with the aid of the functions (20), (21), and (23). The points obtained fell on a curve of the form of (22) in this case also.

LITERATURE CITED

1. F. H. Clauser, "Turbulent boundary layers in adverse pressure gradients," J. Aeronaut. Sci., 21, No. 2 (1954).
2. P. Bradshaw, "A simple method for determining turbulent skin friction from velocity profiles," J. Aero/Space Sci., 26, No. 12 (1959).
3. N. M. Belyanin, "Experimental study of friction and heat exchange during gas flow in a tube," Zh. Prikl. Mekhan. i Tekh. Fiz., No. 4 (1964).
4. Barbin and Jones, "Turbulent flow in the entry region of a smooth tube," Trans. ASME, Ser. D, Tech. Mechan., No. 1 (1963).
5. Olson and Eckert, "Experimental study of turbulent flow in a cylindrical porous tube with uniform gas injection through the walls," Trans. ASME, Ser. E, Appl. Mechan., No. 1 (1966).
6. V. V. Kuz'min, A. A. Tupichenkov, and A. V. Fafurin, "Turbulent boundary layer flow in the entry region of a rough-walled tube," Zh. Prikl. Mekhan. i Tekh. Fiz., No. 5 (1971).
7. A. I. Leont'ev, B. P. Mironov, and A. V. Fafurin, "Experimental study of turbulent heat exchange in the entry and stabilized sections of a cylindrical tube under markedly nonisothermal conditions," Inzh.-Fiz. Zh., 16, No. 4 (1969).
8. L. H. Black and R. F. Cuffel, "Turbulent boundary layer and heat transfer measurements in a convergent–divergent nozzle," Paper ASME, No. HT-4 (1971).
9. Heat and Mass Exchange and Friction in the Turbulent Boundary Layer [in Russian], Siberian Branch, Academy of Sciences of the USSR, Novosibirsk (1964).
10. A. I. Leont'ev, B. P. Mironov, and A. V. Fufurin, "Study of turbulent heat exchange in the entry region of a porous tube under nonisothermal conditions," Teplofiz. Vys. Temp., 7, No. 6 (1969).
11. A. I. Leont'ev, A. V. Fafurin, and P. V. Nikitin, "The turbulent boundary layer in the entry section of a tube under nonisothermal conditions and with injection," Teplofiz. Vys. Temp., 7, No. 2 (1969).
12. A. I. Leont'ev, B. P. Mironov, and A. V. Fafurin, "The turbulent boundary layer in a dissociating gas in the entry section of a tube," Zh. Prikl. Mekhan. i Tekh. Fiz., No. 1 (1967).
13. G. Schlikhting, Boundary-Layer Theory [Russian translation], Nauka, Moscow (1969).